kit (Wako Pure Chemicals Industries, Osaka, Japan). Plasma PAF-AH activity was measured by spectrophotometric assay method [6, 40] utilizing the AZWELL Auto PAF-AH kit (AZWELL Inc., Osaka, Japan). Plasma isoprostane 8,12-iso-iPF(2alpha)-VI was measured by liquid chromatography–electrospray ionization–mass spectrometry as described elsewhere [41].

Immunological detection was performed using standard methods [42] unless otherwise indicated. For fractionation of plasma lipoproteins, pooled plasma samples were subject to fast protein liquid chromatography (FPLC) gel filtration (Pharmacia LKB Biotechnology, Uppsala, Sweden) on a Superose 6 column. Each fraction was collected in 375 μl and the cholesterol concentration and PAF-AH activities were measured. The images of histological examination were captured using the light or fluorescent microscope and subsequently digitized.

Construction of adenoviral vector

A second generation adenoviral vector encoding human plasma PAF-AH cDNA under the control of a CMV promoter, was constructed following the conventional method [6, 43]. In brief, after the human plasma PAF-AH cDNA was subcloned into the shuttle plasmid vector pAdCMV-link [44], this plasmid was linearized and cotransfected into HEK293 cells along with ClaI-digested adenoviral DNA purified from AdLacZ. Cells were overlaid with agar and incubated at 32 °C for 14 days. After confirming the presence of PAF-AH cDNA and the absence of LacZ and wild type adenovirus, the new recombinant adenovirus, designated as AdPAFAH, was propagated with HEK293 cells and purified through ultra-centrifugation utilizing CsCl gradient. AdLacZ was used as a control adenovirus.

Animal experiment

All animal experiments were approved by the University of Tokyo Ethics Committee for Animal Experiments. Imai rats, provided by Takeda pharmaceutical company, were bred and fed a standard laboratory diet and water *ad libitum*. For collection of urine, each rat was housed in an individual metabolic cage for 24 hours under fasting with free access to water prior to and weekly following injection of the adenovirus. Male Imai rats, 12 weeks of age and weighing 450-500g, were grouped on the basis of daily urinary protein excretion to ensure similar urinary protein levels in each group, and injected intravenously with either AdPAFAH or AdLacZ, at a dose of 5×10^{10} pfu per animal, or PBS. Blood sampling was performed from the retro-orbital plexus after 24-hour fasting. Animals were sacrificed 3, 7, 14, or 28 days after injection of the adenovirus under anaesthesia with pentobarbital (40 mg/kg IP), and liver and kidney tissue samples were then embedded in OCT compound or fixed in 10% formalin for histological examination. Aorta samples from some animals were also embedded in OCT compound.

Histological examination

The OCT-embedded kidney, liver and aorta samples were sectioned 6 μm in thickness and mounted on slides. Sections were rapidly dried and fixed in acetone, incubated in methanol/H_2O_2 to inactivate internal peroxidase, and blocked with Blockace (Yukijirushi Nyugyo, Sapporo, Japan). For detection of PAF-AH, sections were reacted with polyclonal rabbit anti-human PAF-AH antibody (Cayman Chemical Co., Ann Arbor, MI, USA). The sections were then incubated with biotinylated goat anti-rabbit IgG, followed by incubation with peroxidase-conjugated biotin-streptavidin complexes. Staining was performed using 3, 3'-diaminobenzidine tetrahydrochloride (DAB) as the substrate; thus antibody reactivity

was noted in a brown color.

Some kidney sections were subjected to additional staining of RECA-1 or Thy-1 in addition to the staining of PAF-AH. For the staining of RECA-1 or Thy-1, sections were further incubated in 0.1M glycine-HCl (pH2.2) and successively in methanol/H_2O_2 to quench the peroxidase activity of peroxidase-conjugated biotin-streptavidin complexes. Sections were reacted with either monoclonal mouse anti–RECA-1 antibody (Cosmo Bio Ltd, Tokyo, Japan) or monoclonal mouse anti–rat Thy-1 antibody (OX-7 monoclonal antibody (BD Phamingen, San Jose, CA, USA)), followed by incubation with biotinylated goat anti-mouse IgG. Color development was performed with DAB/$NiCl_2$ as the substrate; thus antibody reactivity is detected as a purple color for RECA-1 and Thy-1.

To further confirm the localization of PAF-AH protein in the glomeruli, we employed the fluorescent method for immunodetection. Other kidney sections were double-immunolabeled using the polyclonal rabbit anti-human PAF-AH antibody and OX-7 monoclonal antibody. To detect these antibodies, the sections were incubated with Texas Red-conjugated goat anti-rabbit antibody (Jackson Immuno Research Lab, West Grove, PA, USA) and FITC-conjugated rat anti-mouse antibody (Jackson Immuno Research Lab, West Grove, PA, USA), respectively. Slides mounted with sections were washed, wet-mounted, and examined under fluorescent microscopy.

Kidney samples fixed in 10% formalin were embedded in paraffin, sectioned 6 μm in thickness, mounted on slides and subjected to standard PAS staining protocol. To estimate the state of oxidative stress in the kidney, OCT-embedded kidney sections were analyzed using monoclonal mouse anti 4-hydroxy-2-nonenal (HNE) antibody as a primary antibody, and biotinylated goat anti-mouse IgG as a secondary antibody.

In situ hybridization

The cDNA for human PAF-AH or β-galactosidase was subcloned in pSPT18 (Roche Diagnostics, Basel, Switzerland), a transcription vector containing SP6 and T7 promoters on each side of the multiple cloning sites. After linialization of this plasmid at either end of the cDNA, sense and antisense digoxigenin(DIG)-labeled RNA probes were generated by *in vitro* transcription in the presence of DIG-UTP using SP6 and T7 RNA polymerase (Roche Diagnostics), respectively.

The OCT-embedded tissue samples were sectioned 10 μm in thickness, mounted on slides, rapidly dried and fixed in 10% formalin, and pretreated using RiboMap kit (Ventana Japan K.K., Tokyo, Japan). Sections were hybridized with DIG-labeled RNA probes followed by incubation with alkaline phosphatase-conjugated anti-DIG antibody (Roche Diagnostics). These hybridization procedures were performed according to the standard protocol using HX System Discovery (Ventana). Signal detection was performed using NBT / BCIP (Sigma, St.Louis, MO, USA) as the substrate.

Injection of HDL particles

Male Sprague-Dawley rats, 12 weeks of age, were injected intravenously with 5 x 10^{10} pfu of either AdPAFAH or AdLacZ. Three days after injection, the animals were sacrificed and their blood was collected. HDL was isolated from the serum by standard ultracentrifugation, followed by dialysis against PBS and filterization. PAF-AH activity in purified HDL was 3.96 x 10^5 IU/l. The HDL was then injected intravenously into Imai rats for 4 consecutive days in a volume of 1.8ml per daily injection. Animals were sacrificed on Day 5, and the extracted kidney samples were subject to immunohistological examination for

the presence of PAF-AH.

Statistical Analysis

Comparison of data among the experimental groups was carried out using the Student's t-test. Data are expressed as means ± SEM. *P* values less than 0.05 were considered significant.

Acknowledgements

We are greatly indebted to Dr. Akishige Ritani (Ventana Japan K.K.) for technical assistance on in situ hybridization, to Dr. Masaomi Nangaku (Tokyo University) for valuable technical advice, to Dr. Akihide Nakao (Tokyo University) for animal handling, and to Ms. Kaoru Amitani for sectioning the samples. This research was supported in part by the Takeda Science Foundation and a grant-in-aid No.15590931 from Japan Society for the Promotion of Science.

References

1. Diamond, J. R. (1992). The role of reactive oxygen species in animal models of glomerular disease. *Am J Kidney Dis* **19**: 292-300.

2. Catherwood, M. A., Powell, L. A., Anderson, P., McMaster, D., Sharpe, P. C., and Trimble, E. R. (2002). Glucose-induced oxidative stress in mesangial cells. *Kidney Int* **61**: 599-608.

3. Scivittaro, V., Ganz, M. B., and Weiss, M. F. (2000). AGEs induce oxidative stress and activate protein kinase C-beta(II) in neonatal mesangial cells. *Am J Physiol Renal Physiol* **278**: F676-683.

4. Lal, M. A., Brismar, H., Eklof, A. C., and Aperia, A. (2002). Role of oxidative stress in advanced glycation end product-induced mesangial cell activation. *Kidney Int* **61**: 2006-2014.

5. Watson, A. D., *et al.* (1995). Effect of platelet activating factor-acetylhydrolase on the formation and action of minimally oxidized low density lipoprotein. *J Clin Invest* **95**: 774-782.

6. Noto, H., *et al.* (2003). Human plasma platelet-activating factor acetylhydrolase binds to all the murine lipoproteins, conferring protection against oxidative stress. *Arterioscler Thromb Vasc Biol* **23**: 829-835.

7. Quarck, R., *et al.* (2001). Adenovirus-mediated gene transfer of human platelet-activating factor-acetylhydrolase prevents injury-induced neointima formation and reduces spontaneous atherosclerosis in apolipoprotein E-deficient mice. *Circulation* **103**: 2495-2500.

8. Tanaka, R., *et al.* (1999). Role of platelet-activating factor acetylhydrolase gene mutation in Japanese childhood IgA nephropathy. *Am J Kidney Dis* **34**: 289-295.

9. Yoon, H. J., *et al.* (2002). Interdependent effect of angiotensin-converting enzyme and platelet-activating factor acetylhydrolase gene polymorphisms on the progression of immunoglobulin A nephropathy. *Clin Genet* **62**: 128-134.

10. Imai, Y., and Matsumura, H. (1973). Genetic studies on induced and spontaneous hypercholesterolemia in rats. *Atherosclerosis* **18**: 59-64.

11. Imai, Y., Matsumura, H., Miyajima, H., and Oka, K. (1977). Serum and tissue lipids and glomerulonephritis in the spontaneously hypercholesterolemic (SHC) rat, with a note on the effects of gonadectomy. *Atherosclerosis* **27**: 165-178.

12. Kondo, S., Yoshizawa, N., and Wakabayashi, K. (1995). Natural history of renal lesions in spontaneously hypercholesterolemic (SHC) male rats. *Nippon Jinzo Gakkai Shi* **37**: 91-99.

13. Sato, T., Liang, K., and Vaziri, N. D. (2002). Down-regulation of lipoprotein lipase and VLDL receptor in rats with focal glomerulosclerosis. *Kidney Int* **61**: 157-162.

14. Imai, E., and Isaka, Y. (1998). Strategies of gene transfer to the kidney. *Kidney Int* **53**: 264-272.

15. Tsukamoto, K., Tangirala, R., Chun, S. H., Pure, E., and Rader, D. J. (1999). Rapid regression of atherosclerosis induced by liver-directed gene transfer of ApoE in ApoE-deficient mice. *Arterioscler Thromb Vasc Biol* **19**: 2162-2170.

16. Tsujie, M., Isaka, Y., Nakamura, H., Kaneda, Y., Imai, E., and Hori, M. (2001). Prolonged transgene expression in glomeruli using an EBV replicon vector system combined with HVJ liposomes. *Kidney Int* **59**: 1390-1396.

17. Heikkila, P., Parpala, T., Lukkarinen, O., Weber, M., and Tryggvason, K. (1996). Adenovirus-mediated gene transfer into kidney glomeruli using an ex vivo and in vivo kidney perfusion system - first steps towards gene therapy of Alport syndrome. *Gene Ther* **3**: 21-27.

18. Imai, E., Takabatake, Y., Mizui, M., and Isaka, Y. (2004). Gene therapy in renal diseases. *Kidney Int* **65**: 1551-1555.

19. Tsaoussis, V., and Vakirtzi-Lemonias, C. (1994). The mouse plasma PAF acetylhydrolase: II. It consists of two enzymes both associated with the HDL. *J Lipid Mediat Cell Signal* **9**: 317-331.

20. Stafforini, D. M., *et al.* (1999). Molecular basis of the interaction between plasma platelet-activating factor acetylhydrolase and low density lipoprotein. *J Biol Chem* **274**: 7018-7024.

21. Stafforini, D. M., McIntyre, T. M., Carter, M. E., and Prescott, S. M. (1987). Human plasma platelet-activating factor acetylhydrolase. Association with lipoprotein particles and role in the degradation of platelet-activating factor. *J Biol Chem* **262**: 4215-4222.

22. Gonzalez-Rubio, M., Voit, S., Rodriguez-Puyol, D., Weber, M., and Marx, M. (1996). Oxidative stress induces tyrosine phosphorylation of PDGF alpha-and beta-receptors and pp60c-src in mesangial cells. *Kidney Int* **50**: 164-173.

23. Kamanna, V. S., Bassa, B. V., Vaziri, N. D., and Roh, D. D. (1999). Atherogenic lipoproteins and tyrosine kinase mitogenic signaling in mesangial cells. *Kidney Int Suppl* **71**: S70-75.

24. Jenkins, A. J., *et al.* (2000). Native and modified LDL activate extracellular signal-regulated kinases in mesangial cells. *Diabetes* **49**: 2160-2169.

25. Kamanna, V. S. (2002). Low density lipoproteins and mitogenic signal transduction processes: role in the pathogenesis of renal disease. *Histol Histopathol* **17**: 497-505.

26. Lee, H. S., Kim, B. C., Kim, Y. S., Choi, K. H., and Chung, H. K. (1996). Involvement of oxidation in LDL-induced collagen gene regulation in mesangial cells. *Kidney Int* **50**: 1582-1590.

27. Roh, D. D., Kamanna, V. S., and Kirschenbaum, M. A. (1998). Oxidative modification of low-density lipoprotein enhances mesangial cell protein synthesis and gene expression of extracellular matrix proteins. *Am J Nephrol* **18**: 344-350.

28. Iglesias-De La Cruz, M. C., *et al.* (2001). Hydrogen peroxide increases extracellular matrix mRNA through TGF-beta in human mesangial cells. *Kidney Int* **59**: 87-95.

29. Kamanna, V. S., Pai, R., Roh, D. D., and Kirschenbaum, M. A. (1996). Oxidative modification of low-density lipoprotein enhances the murine mesangial cell cytokines associated with monocyte migration, differentiation, and proliferation. *Lab Invest* **74**: 1067-1079.

30. Khachigian, L. M., Collins, T., and Fries, J. W. (1997). N-acetyl cysteine blocks mesangial VCAM-1 and NF-kappa B expression in vivo. *Am J Pathol* **151**: 1225-1229.

31. Massy, Z. A., Kim, Y., Guijarro, C., Kasiske, B. L., Keane, W. F., and O'Donnell, M. P. (2000). Low-density lipoprotein-induced expression of interleukin-6, a marker of human mesangial cell inflammation: effects of oxidation and modulation by lovastatin. *Biochem Biophys Res Commun* **267**: 536-540.

32. Mattana, J., Margiloff, L., and Singhal, P. C. (1997). Metal-catalyzed oxidation of extracellular matrix proteins disrupts integrin-mediated adhesion of mesangial cells. *Biochem Biophys Res Commun* **233**: 50-55.

33. Mattana, J., Margiloff, L., and Chaplia, L. (1999). Oxidation of extracellular matrix modulates susceptibility to degradation by the mesangial matrix metalloproteinase-2. *Free Radic Biol Med* **27**: 315-321.

34. Fernando, R. L., Varghese, Z., and Moorhead, J. F. (1998). Differential ability of cells to promote oxidation of low density lipoproteins in vitro. *Clin Chim Acta* **269**: 159-173.

35. Sharma, P., *et al.* (1996). Native and oxidized low density lipoproteins modulate mesangial cell apoptosis. *Kidney Int* **50**: 1604-1611.

36. Galle, J., Heermeier, K., and Wanner, C. (1999). Atherogenic lipoproteins, oxidative stress, and cell death. *Kidney Int Suppl* **71**: S62-65.

37. Ishikawa, Y., Yokoo, T., and Kitamura, M. (1997). c-Jun/AP-1, but not NF-kappa B, is a mediator for oxidant-initiated apoptosis in glomerular mesangial cells. *Biochem Biophys Res Commun* **240**: 496-501.

38. Wang, J. S., Ger, L. P., and Tseng, H. H. (1997). Expression of glomerular antioxidant enzymes in human glomerulonephritis. *Nephron* **76**: 32-38.

39. Sandau, K., Pfeilschifter, J., and Brune, B. (1998). Nitrosative and oxidative stress induced heme oxygenase-1 accumulation in rat mesangial cells. *Eur J Pharmacol* **342**: 77-84.

40. Kosaka, T., *et al.* (2000). Spectrophotometric assay for serum platelet-activating factor acetylhydrolase activity. *Clin Chim Acta* **296**: 151-161.

41. Ohashi, N., and Yoshikawa, M. (2000). Rapid and sensitive quantification of 8-isoprostaglandin F2alpha in human plasma and urine by liquid chromatography-electrospray ionization mass spectrometry. *J Chromatogr B Biomed Sci Appl* **746**: 17-24.

42. Harlow, E., and Lane, D., Antibodies, A Laboratory Manual., ed., Cold Spring Harbor Laboratory Press,, New York. 1988.

43. Tsukamoto, K., Smith, P., Glick, J. M., and Rader, D. J. (1997). Liver-directed gene transfer and prolonged expression of three major human ApoE isoforms in ApoE-deficient mice. *J Clin Invest* **100**: 107-114.

44. Ye, X., Robinson, M. B., Batshaw, M. L., Furth, E. E., Smith, I., and Wilson, J. M. (1996). Prolonged metabolic correction in adult ornithine transcarbamylase-deficient mice with adenoviral vectors. *J Biol Chem* **271**: 3639-3646.

Figure Legends

Figure 1. Plasma PAF-AH activity and 8,12-iso-iPF(2alpha)-VI (8-epi PGF2α) levels after adenovirus-mediated gene transfer. (**A**) Changes in plasma PAF-AH activity after injection of AdPAFAH (diamonds) (n = 9 until Day 14, and n = 6 after Day 21), AdLacZ (squares) (n = 9 until Day 14, and n = 6 after Day 21), or PBS (circles) (n = 4). (**B**) Distribution of PAF-AH activity on lipoprotein particles 3 days after injection of AdPAFAH. Each fraction fractionated by FPLC was subjected to measurement of TC (squares) or PAF-AH activity (diamonds). (**C**) Time course changes in plasma 8-epi PGF2α levels after injection of AdPAFAH (diamonds) (n = 9 until Day

14, and $n = 6$ after Day 21), AdLacZ (squares) ($n = 9$ until Day 14, and $n = 6$ after Day 21), or PBS (circles) ($n = 4$). **: $P < 0.001$ and *: $P < 0.05$ compared with the other groups on the same day.

Figure 2. Changes in daily urine protein levels after injection of adenoviruses. (Diamonds): AdPAFAH ($n = 9$ until Day 14, and $n = 6$ after Day 21); (squares): AdLacZ ($n = 9$ until Day 14, and $n = 6$ after Day 21); (circles): PBS ($n = 4$). †: $P < 0.01$ and *: $P < 0.05$ compared to other groups on the same day.

Figure 3. Representative immunohistological analysis of liver and kidney samples of Imai rats. Tissue samples were subjected to hPAF-AH immunostaining. **(A-D)** liver specimens from rats injected with AdPAFAH on Day 0 (A), Day 3 (B), Day 7 (C), and Day 28 (D). **(E-H)** kidney specimens from rats injected with AdPAFAH on Day 0 (E), Day 3 (F), Day 7 (G), and Day 28 (H).

Figure 4. Immunostaining of kidney and aorta samples. **(A-E)** samples subjected to hPAFAH immunostaining. A and B: kidney specimens from Imai rats injected with AdLacZ (A) or AdPAFAH (B) on Day 7 (low magnification). Black arrowheads indicate glomeruli, and red arrowheads indicate small arterioles. C: kidney specimen from Imai rats injected with HDL particles abundant in hPAFAH. D and E: thoracic aorta samples from Imai rats injected with AdLacZ (D) or AdPAFAH (E) on Day 7. **(F,G)** double staining (utilizing color detection) of kidney samples on Day 7 for PAF-AH (brown color) and RECA-1 (purple color) (F) or PAF-AH (brown color) and Thy-1 (purple color) (G). **(H-J)** double staining of kidney samples on Day 7 utilizing the fluorescent method. Sample was stained for Thy-1 (H, green) and hPAFAH (I, red), and the images were merged.

Figure 5. Analysis of liver and kidney samples of Imai rats by *in situ* hybridization. **(A)** liver specimen of rats 3 days post-injection of AdLacZ. **(B)** liver specimen of rats 3 days post-injection of AdPAFAH. **(C,D)** kidney specimens of rats injected with AdPAFAH on Day 3 (C) and Day 7 (D). Arrowheads indicate glomeruli.

Figure 6. HNE immunostaining and PAS staining of kidney samples. **(A,B)** HNE immunostaining of specimens from Imai rats injected with AdLacZ on Day 14 (A) or AdPAFAH on Day 14 (B). Arrowheads indicate glomeruli. **(C,D)** PAS staining of specimens from rats injected with AdLacZ on Day 28 (C) or AdPAFAH on Day 28 (D).

Figure 1

A

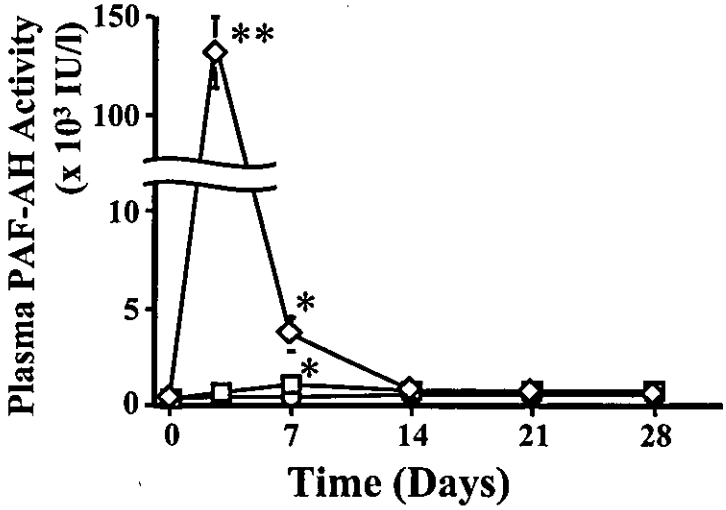
Plasma PAF-AH Activity
(x 10³ IU/l)
150
100
10
5
0
**
*
*
0
7
14
21
28
Time (Days)

B

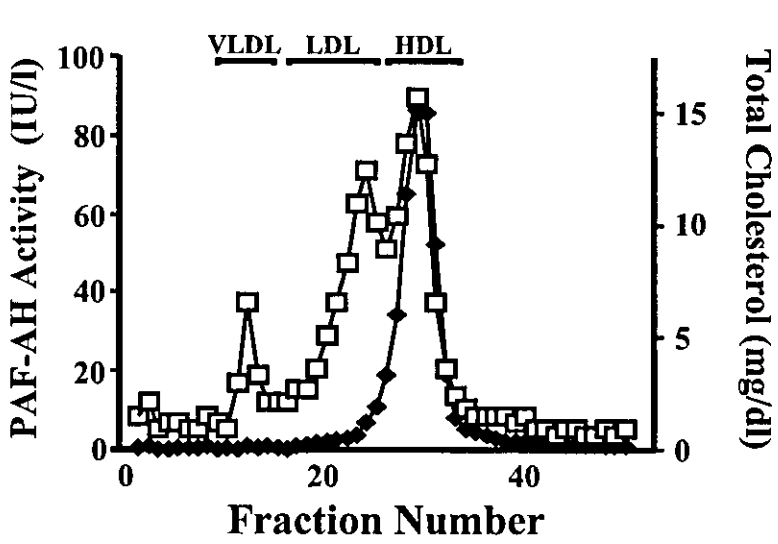
VLDL
LDL
HDL
PAF-AH Activity (IU/l)
100
80
60
40
20
0
Total Cholesterol (mg/dl)
15
10
5
0
0
20
40
Fraction Number

C

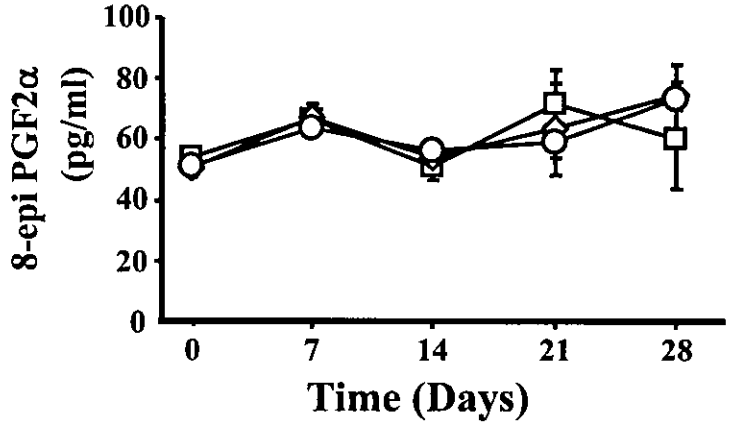
8-epi PGF2α
(pg/ml)
100
80
60
40
20
0
0
7
14
21
28
Time (Days)

Figure 2

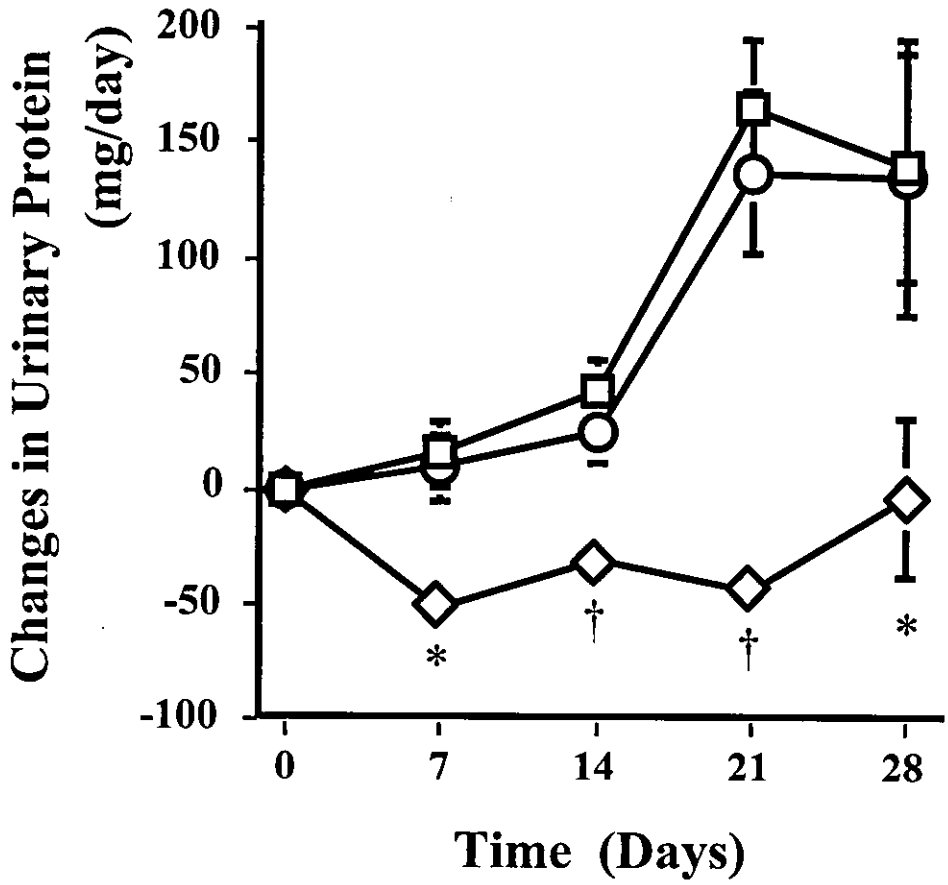
Changes in Urinary Protein
(mg/day)
200
150
100
50
0
-50
-100
0
7
14
21
28
Time (Days)
*
†
†
*

Figure 3

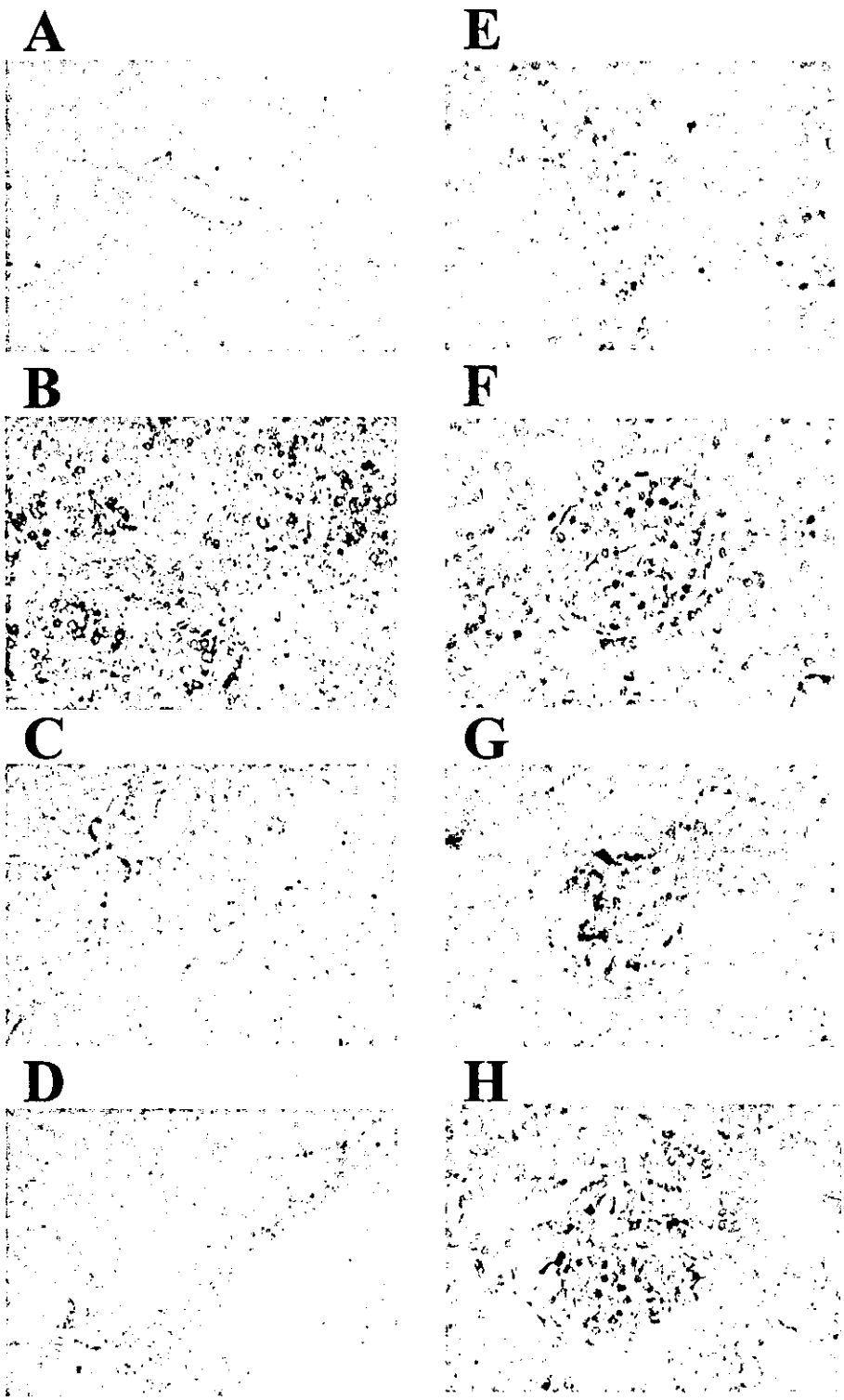

Figure 4

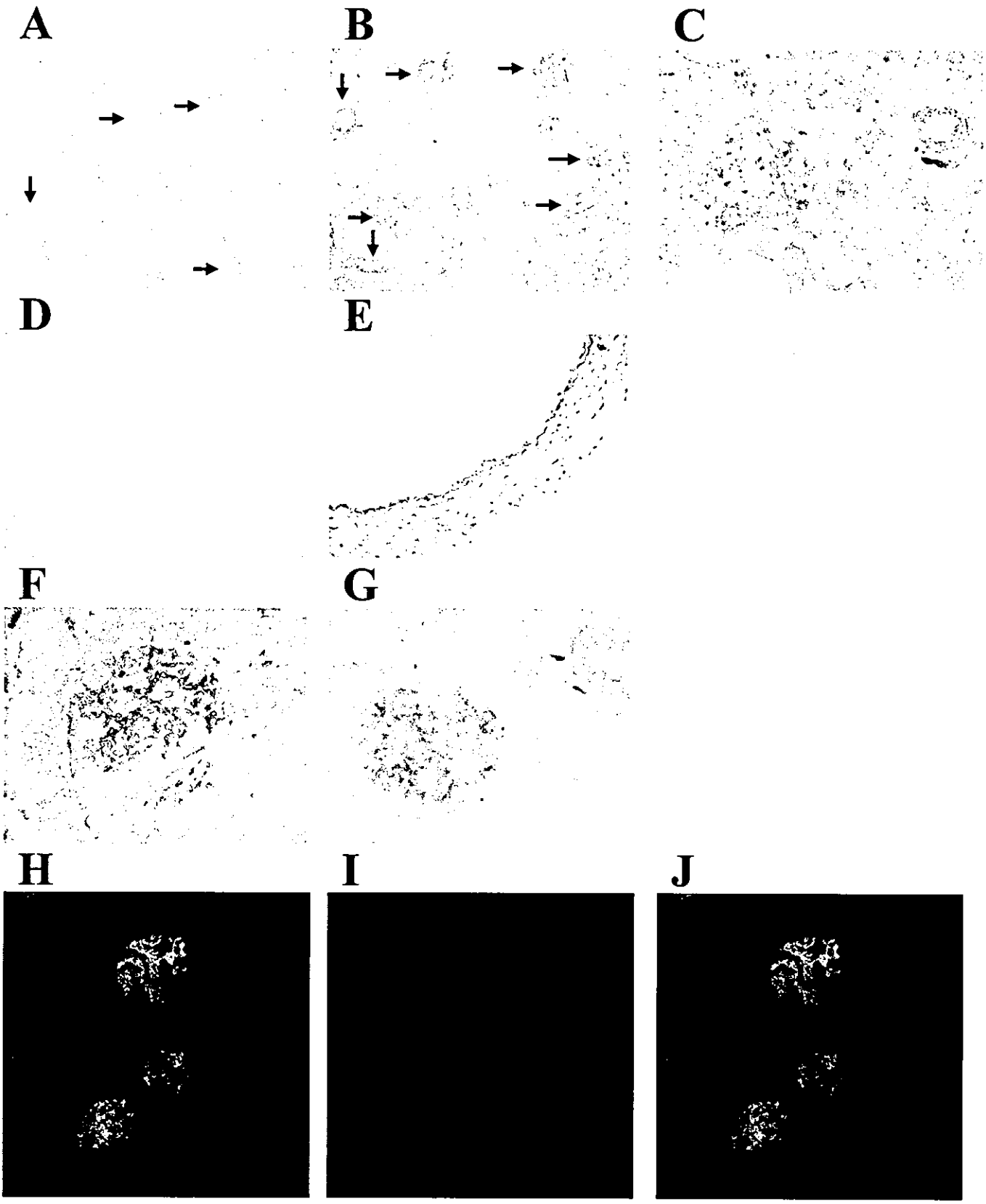

Figure 5

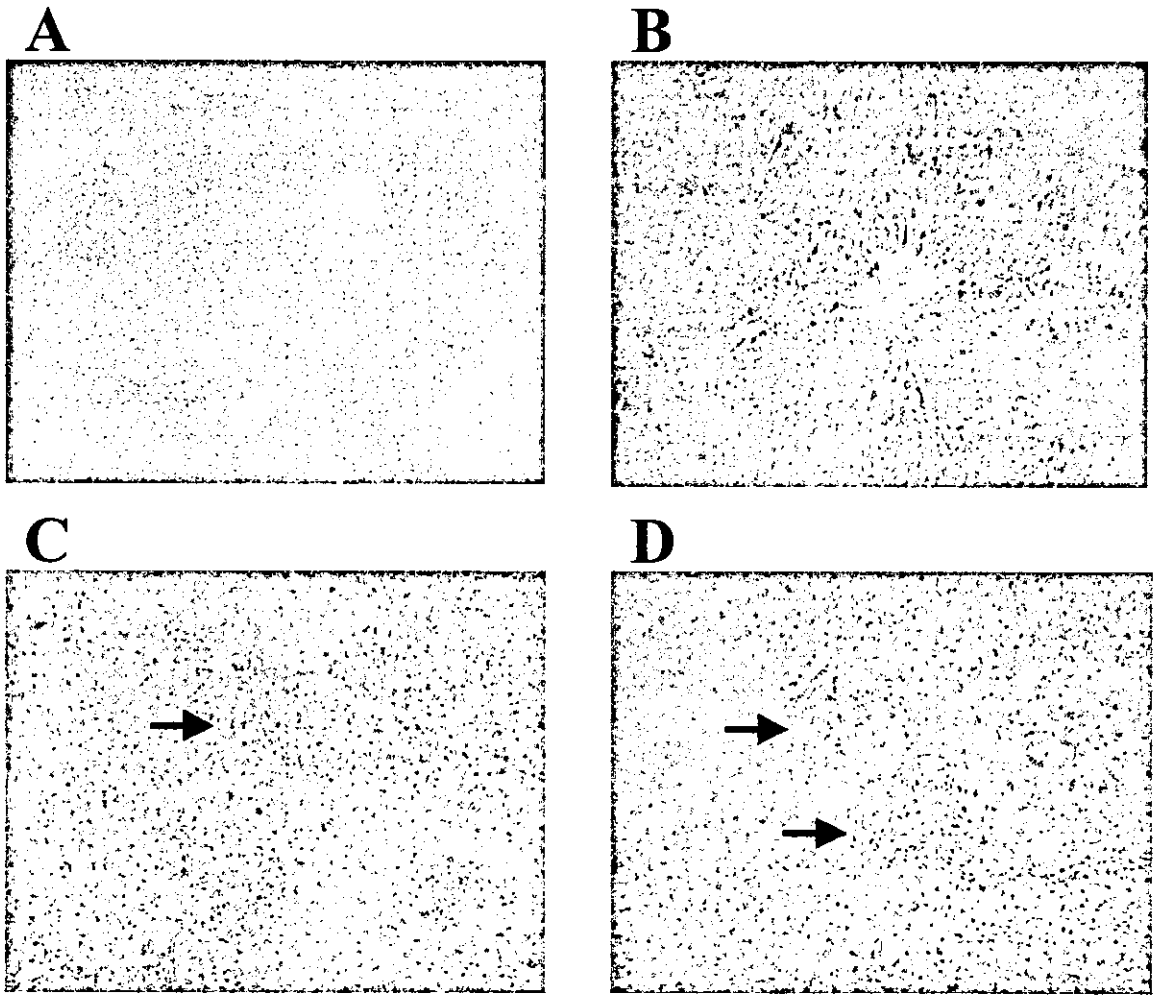

Figure 6

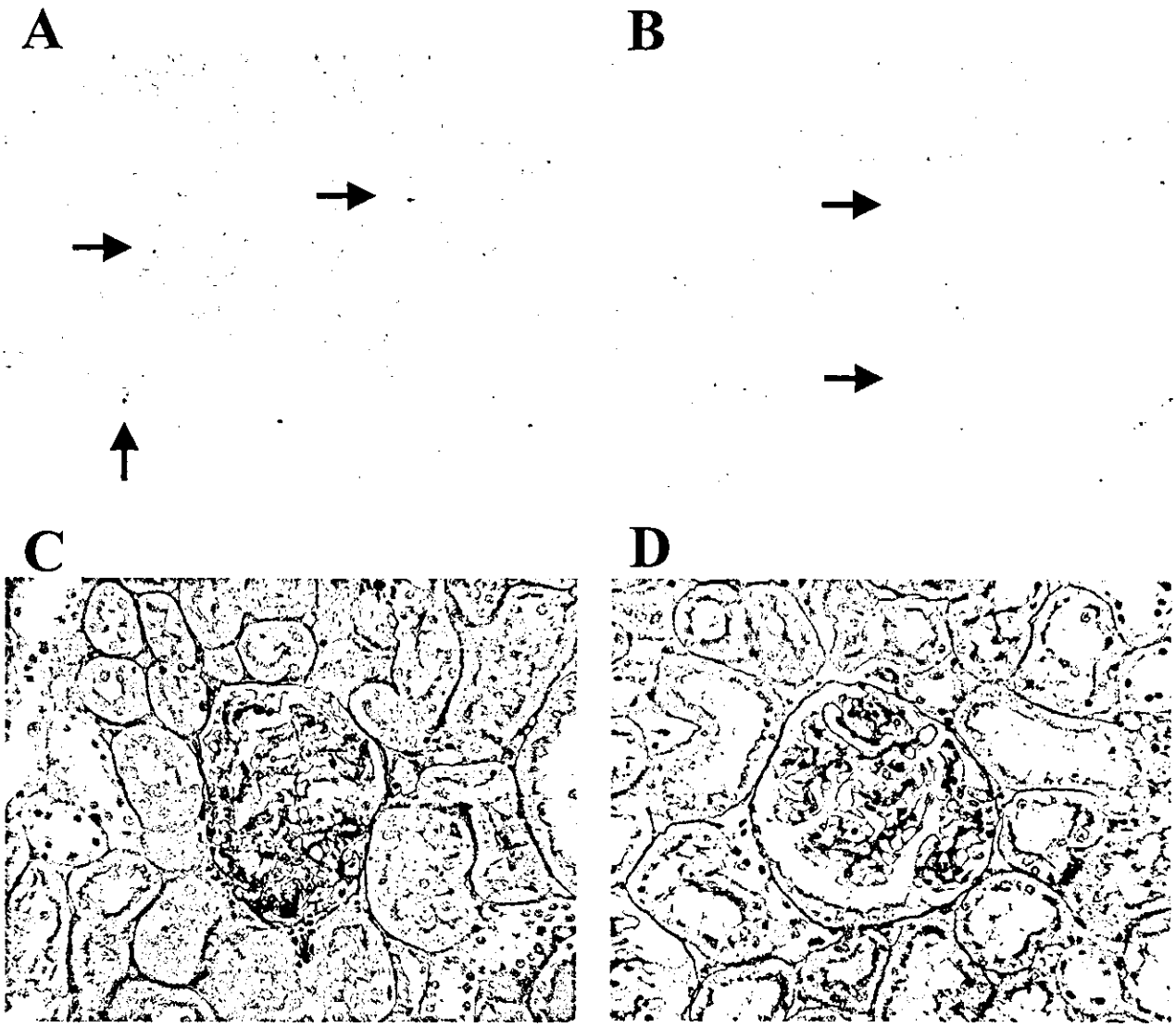

ELSEVIER

Journal of Hepatology 42 (2005) 110–116

Journal of Hepatology

www.elsevier.com/locate/jhep

Involvement of mitochondrial permeability transition in acetaminophen-induced liver injury in mice

Yasuhiro Masubuchi, Chieko Suda, Toshiharu Horie*

Department of Biopharmaceutics, Graduate School of Pharmaceutical Sciences, Chiba University, 1-8-1 Inohana, Chuo-ku, Chiba 260-8675, Japan

***Background/Aims*: Although mitochondria have been demonstrated as primary targets in acetaminophen hepatotoxicity, the mechanism for mitochondria-mediated toxicity has not been defined. We examined the role of mitochondrial permeability transition (MPT) in the acetaminophen-induced liver injury.**

***Methods*: Male CD-1 mice were given intraperitoneally acetaminophen (350 mg/kg) without or with cyclosporin A (50 mg/kg), a specific inhibitor of MPT. Serum alanine aminotransferase (ALT), a marker of liver injury, and other biochemical parameters were determined.**

***Results*: Acetaminophen-induced ALT leakage was attenuated by co-administration of cyclosporin A. Cyclosporin A did not affect acetaminophen-induced early decrease in hepatic reduced glutathione (GSH) contents, indicating lack of the effect on the metabolic activation. Acetaminophen-induced decrease in mitochondrial GSH and ATP contents, and cytosolic leakage of cytochrome c were attenuated by cyclosporin A, suggesting that mitochondrial oxidative stress and ATP depletion resulting from MPT are principle mechanisms involved in acetaminophen-induced liver injury. Mitochondrial swelling by calcium was exacerbated in the mitochondria isolated from the acetaminophen-treated mice. In vitro exposure of intact mitochondria to *N*-acetyl-*p*-benzoquinone imine (NAPQI) with calcium caused mitochondrial swelling.**

***Conclusions*: The present data indicate that the MPT is the principal mechanism in the acetaminophen-induced liver injury and NAPQI is a candidate to open the transition pore.**

***Keywords*: Acetaminophen; Liver injury; Mitochondrial permeability transition; Cyclosporin A; Glutathione; ATP; Cytochrome c; *N*-Acetyl-*p*-benzoquinone imine**

1. Introduction

An overdose of the analgesic drug acetaminophen causes liver injury in experimental animals and humans. The toxicity has been shown to be initiated by cytochrome P450 metabolism to *N*-acetyl-*p*-benzoquinone imine (NAPQI) [1,2]. The high reactivity of NAPQI with sulfhydryl groups results in depleting glutathione in hepatocytes, followed by covalent binding to intracellular proteins [3,4]. Although it has been shown that the relative amount of covalent binding is correlated with the development of the toxicity [3], it is also suggested that the covalent binding is not sufficient for the toxicity [5–7]. Extensive studies were thus focused on covalent binding to specific protein(s) as a trigger of the toxicity. A number of proteins have been identified as targets of NAPQI by the immunological techniques [8] and recent proteomics [9]. Because development of various mitochondria dysfunctions has been observed with acetaminophen toxicity, which include inhibition of respiration, a decrease in hepatic ATP levels, a decrease in membrane potential, a loss of mitochondrial Ca^{2+} [10–13], it was proposed that mitochondria was primary target of the reactive metabolite. Indeed, some of the target proteins were localized in mitochondria fraction including glutamate dehydrogenase, aldehyde dehydrogenase, carbamyl phosphate synthetase-I and ATP synthetase α-subunit [8,9]. These enzyme activities in the mitochondrial fraction were decreased partially [14,15], probably as consequences of covalent binding, while it is

Received 27 April 2004; received in revised form 16 September 2004; accepted 21 September 2004; available online 12 October 2004

* Corresponding author. Tel./fax: +81 43 226 2886.
E-mail address: horieto@p.chiba-u.ac.jp (T. Horie).

0168-8278/$30.00
doi:10.1016/j.jhep.2004.09.015

also estimated that only the loss of the any single enzyme activity could not explain mitochondria-mediated acetaminophen hepatotoxicity. It is thus presumed that the toxicity is accounted for by combination of covalent binding to several functional proteins and/or by secondary event following the covalent binding.

Mitochondrial permeability transition (MPT) is recently focused as a mechanism for drug-induced hepatocyte injury [16–18]. The MPT represents an abrupt increase in permeability of the mitochondrial inner membrane to allow solutes with a molecular weight less than 1500 [19]. The MPT is promoted by the accumulation of excessive Ca^{2+} and stimulated by various compounds and conditions. It leads to dissipation of membrane potential ($\Delta\psi$), uncoupling of oxidative phosphorylation, loss of pre-accumulated Ca^{2+}, and expansion of the matrix volume. MPT causes both apoptotic and necrotic cell death. Acetaminophen could induce hepatocyte apoptosis in vitro as well as necrosis [16,17], whereas the quantitative determination of cell death after exposure of hepatotoxic dose of acetaminophen in vivo indicated that acetaminophen caused extensively oncotic necrosis rather than apoptosis [20]. Recent papers proposed the possibility of MPT as a mechanism for acetaminophen-induced liver injury [21,22], but have not been fully supported by experimental data. In the present study, we investigated the possible involvement of MPT in acetaminophen-induced liver injury in male CD-1 mice by using a MPT specific inhibitor, cyclosporin A.

2. Materials and methods

2.1. Chemicals

Acetaminophen and NAPQI were purchased from Sigma-Aldrich (St Louis, MO); cyclosporin A, glutathione, reduced form (GSH) and glutathione disulfide (GSSG) were from the Wako Pure Chemical Ind. (Osaka, Japan); ATP was from Oriental Yeast Co., Ltd (Tokyo, Japan). All other chemicals and solvents were of analytical grade.

2.2. Animals and in vivo treatment

Male CD-1 mice were purchased from Takasugi Experimental Animals (Saitama, Japan). The mice were used in the experiment at the age of 8–9 weeks. The mice were acclimatized at least 1 week in a climate-controlled room on a 12-hour light-dark cycle and were fed ad libitum. All procedures and care were carried out according to the National Institutes of Health Guide for the Care and Use of Laboratory animals. The mice were then fasted for 16 h before experiments to sensitize mice to acetaminophen toxicity by decreasing basal levels of liver GSH. Mice received intraperitoneally (i.p.) 10-ml/kg saline or 350 mg/kg of acetaminophen. In some experiments, mice received 10-ml/kg i.p. corn oil or cyclosporin A (50 mg/kg) in the oil just before saline or acetaminophen. Two, 8 or 24 h after the treatment, blood of the mice was collected and the mice were killed to obtain their livers. A portion of the liver was fixed in 10% buffered formalin for histological sections. The blood was allowed to coagulate and the samples were then centrifuged to obtain the serum. In some experiments, the bile duct was cannulated with polyethylene tubing (PE 10) to allow sampling of bile and the bile was collected for 15 min.

2.3. Assessment of hepatotoxicity

Serum alanine aminotransferase (ALT) activities were assayed as a marker of acetaminophen-induced hepatotoxicity. Assays were run on the test kit (Sigma Diagnostics, St Louis, MO). Formalin-fixed tissue sections were embedded in paraffin, mounted onto glass slides, and stained with hematoxylin–eosin (Takasaki Pathologic Center, Gunma, Japan). Hepatotoxicity was also assessed by histological examination of the tissue sections.

2.4. Isolation of liver mitochondria

Liver mitochondrial fraction was prepared according to the method described by Schneider and Hogeboom [23] with modifications. The livers were isolated and placed in the ice-cold medium containing 250 mM sucrose, 10 mM HEPES-KOH, pH 7.4, and 0.5 mM EGTA. The livers were cut to small cubes with scissors in 50 ml of the medium and homogenized five times in a Potter homogenizer. The homogenates were diluted to 100 ml per liver and were centrifuged at $770\times g$ for 5 min kept at 4 °C. The resulting supernatant was decanted and further centrifuged at $9800\times g$ for 10 min. The supernatant was discarded, the pellet was suspended in 20 ml of the ice-cold isolation medium, and centrifuged at $4500\times g$ for 10 min. The final mitochondrial pellet was suspended in 1 ml of medium containing 250 mM sucrose and 10 mM HEPES-KOH, pH 7.4. Protein concentration of the mitochondrial fraction was determined by the method of Lowry et al. [24].

2.5. Assay of GSH and GSSG

GSH and GSSG contents in liver homogenates, mitochondria and bile were determined by an HPLC method according to Keller and Menzel [25] with modifications. The reaction medium (1.0 ml) was mixed with 0.5 ml solution consisting of 5% metaphosphoric acid/0.1% EDTA (2:7, v/v). The sample was centrifuged ($16{,}000\times g$, 5 min) and the supernatant (0.5 ml) mixed with 10 ml of 250 mM 3-fluorotyrosine as an internal standard for HPLC. The samples were applied after filtration to the HPLC column (Inertsil ODS, GL Sciences Inc., Tokyo). The mobile phase consisting of 0.1% trifluoroacetic acid/methanol (9/1, v/v) was pumped at a flow rate of 1.0 ml/min. The effluent from the column was mixed with luminescence reagent consisting of 18.6 mM o-phthalaldehyde and 17.1 mM 2-mercaptoethanol pumped at a flow rate of 0.2 ml/min. The fluorescence intensity at the 355/425 nm wavelength pair was monitored.

2.6. Assay of mitochondrial ATP content

Liver mitochondria were suspended into 0.5 ml of 1N $HClO_4$ and disrupted by vortex mixing with the acid. After the neutralization with 2N KOH, the sample was centrifuged ($16{,}000\times g$, 30 s) and supernatant was used for assay for ATP. ATP content was measured with Sigma ATP bioluminescent assay kit based on the luciferin-luciferase method by a chemiluminescence analyzer.

2.7. Detection of cytochrome c in cytosol

Cytochrome c in hepatic cytosol fraction was detected by immunoblot analysis. Cytosolic proteins (5.0 μg) were separated by SDS–PAGE with a 15% polyacrylamide gel. The proteins on the gel were transferred to a polyvinylidine difluoride membrane (Bio-Rad Laboratories, Hercules, CA, USA). The membrane was treated with the anti-cytochrome c antibody (clone 7H8.2C12, Lab Vision Co., Fremont, CA), which was diluted 1:1000 for use. The immunoblots were developed with the enhanced chemiluminescence detection method with reagents from Amersham Pharmacia Biotech (Uppsala, Sweden), according to the manufacturer's instructions.

2.8. Incubation of mitochondria

Reaction medium containing 1.0 mg/ml liver mitochondrial protein, 125 mM sucrose, 150 mM KCl, 10 mM HEPES-KOH, and 2.5 μM

rotenone was preincubated at 30 °C. The liver mitochondria from acetaminophen-treated or control mice were energized by 5 mM succinate. The incubation was started by adding 20 μM $CaCl_2$ and was performed at 30 °C for various time periods. In the experiment to determine in vitro effects of acetaminophen and NAPQI, the liver mitochondria from untreated mice in the above-mentioned mixture with 20 μM $CaCl_2$ were energized by 5 mM succinate. The incubation was started by adding acetaminophen or NAPQI and was performed at 30 °C for various time periods. In some experiments, the mixture included 1 μM cyclosporin A.

2.9. Assessment of mitochondrial permeability transition

Mitochondrial swelling as the indicator of MPT was estimated from the decrease in absorbance at 540 nm.

2.10. Assessment of mitochondrial membrane potential

The electrical transmembrane potential of mitochondria was monitored spectrophotometrically with the cationic dye, rhodamine 123 at the concentration of 0.5 μM. After the 2-min preincubation with succinate, incubation was started by the addition of acetaminophen or NAPQI and was performed for 3 min. The reaction medium was immediately centrifuged (16,000×*g*, 30 s) and fluorescence intensity of the supernatant was monitored at the 505/535 nm wavelength pair. $\Delta\psi$ was calculated by the Nernst equation as described previously [26].

2.11. Statistical analysis

The experimental groups were compared by analysis of variance, followed by Newman–Keuls multiple comparisons test to determine significant differences between the group means.

3. Results

3.1. Protection of mice from acetaminophen-induced liver injury by cyclosporin A

Administration of acetaminophen (350 mg/kg) to male CD-1 mice induced an increase in serum ALT leakage at 8 and 24 h after the injection (Table 1). No significant increase in ALT was observed 2 h after the treatment (data not shown). The ALT leakage was significantly suppressed by co-administration of cyclosporin A (50 mg/kg, i.p.), a typical inhibitor of MPT pore opening, suggesting that MPT is involved in pathogenesis of the acetaminophen-induced liver injury. Cyclosporin A itself was not hepatotoxic under the present condition. Moreover,

Table 1
Effect of cyclosporin A on acetaminophen-induced liver injury

	$ALT_{8\,h}$ (IU/l)	$ALT_{24\,h}$ (IU/l)
Control	12±1	16±4
Cyclosporin A	17±3	11±3
Acetaminophen	1765±541*	2459±548**
Cyclosporin A + acetaminophen	396±291#	986±260**#

Mice were given acetaminophen (350 mg/kg, i.p.) together with or without cyclosporin A (50 mg/kg, i.p.), and were killed at 8 or 24 h after the treatment. The results are means±SE of 6–12 mice. *$P<0.05$, **$P<0.01$, Significantly different from corresponding control. #$P<0.05$, Significantly different from 'Acetaminophen' group.

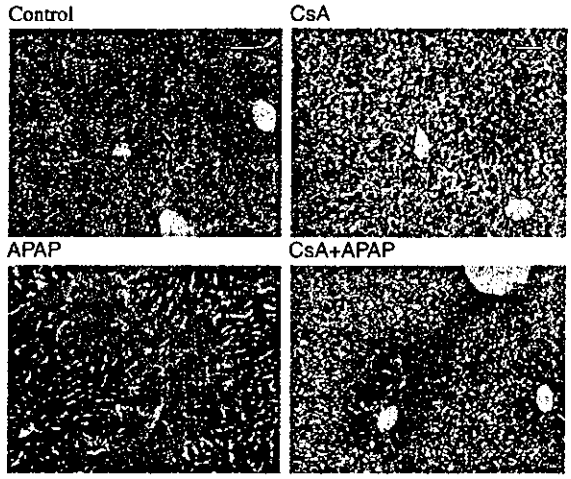

Fig. 1. Histopathology of liver 24 h after administration of acetaminophen. Mice were given acetaminophen (APAP, 350 mg/kg, i.p.) together with or without cyclosporin A (CsA, 50 mg/kg, i.p.), and were killed 24 h after the treatment. Liver sections were subjected to hematoxylin–eosin staining.

histological examination of liver tissues 24 h after treatment with acetaminophen revealed centrilobular necrosis with hemorrhage, whereas the mice treated together with cyclosporin A showed only minimal hepatic necrosis (Fig. 1).

Acetaminophen-induced liver injury is mediated by its reactive metabolite, NAPQI. NAPQI binds to GSH, resulting in depleting hepatic GSH, followed by covalently binding to cellular critical targets. Therefore, an early decrease in hepatic GSH is the reflect of NAPQI formation. The hepatic GSH level markedly decreased 2 h after the acetaminophen treatment, and the decrease was not affected by the coadministration with cyclosporin A (Fig. 2). Similar results were obtained when measured at an earlier time point (30 min; acetaminophen, 2.96±0.71; acetaminophen+cyclosporin A, 3.24±0.38 nmol/mg protein). The unchanged depletion rate of GSH suggests that the production of NAPQI is not affected by cyclosporin A at

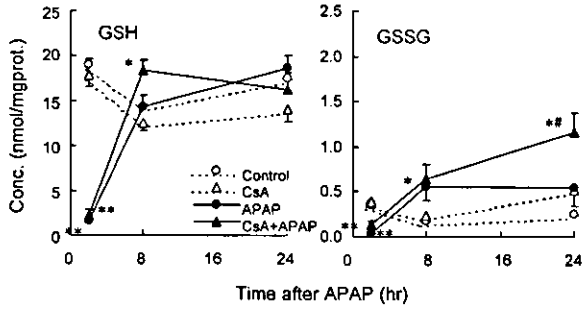

Fig. 2. Time course of hepatic GSH and GSSG contents after administration of acetaminophen. Mice were given acetaminophen (APAP, 350 mg/kg, i.p.) together with or without cyclosporin A (CsA, 50 mg/kg, i.p.), and were killed at various time points. Contents of GSH and GSSG in liver homogenates were determined. The results are means±SE of 3–6 mice. *$P<0.05$, **$P<0.01$, Significantly different from corresponding APAP(−) groups.

least under these experimental conditions. Cyclosporin A is a substrate of CYP3A [27]. While NAPQI formation is mediated mainly by CYP2E1 in mice [28], several reports indicated that other P450 isozymes including CYP3A also contributed to the metabolism [29,30]. Thus, it may be possible for cyclosporin A to inhibit CYP3A-dependent NAPQI generation.

Similar early decrease was also obtained for GSSG (Fig. 2). Because GSH is oxidized to form GSSG, the decrease in GSSG would be associated with the depletion of GSH. The hepatic GSH level was completely recovered 8 h after the injection, whereas hepatic GSSG levels were increased as compared to controls and, furthermore, cyclosporin A potentiated this effect at the later time point (Fig. 2). It is considered that the increases in GSSG is accounted for the oxidative stress secondary to acetaminophen-induced liver injury [21] and by the additional effects of cyclosporin A, which is known to induce oxidative stress [31].

3.2. Changes in mitochondrial parameters in the mice with acetaminophen-induced liver injury

Although, the GSH content in liver homogenate was returned to the control level 8 h after the acetaminophen treatment (Fig. 2), the content in the mitochondria fraction was lower than control at the same time point. Furthermore, mitochondrial GSSG content markedly increased in the treated mice (Fig. 3). These results indicate mitochondrial oxidative stress, which plays an important role in initiation of the acetaminophen hepatotoxicity [32]. The collapse of the mitochondrial redox balance was partially prevented by cyclosporin A (Fig. 3). Similar results were obtained 24 h after the treatment (data not shown). Therefore, increase in tissue GSSG levels observed at 24h after the treatment with cyclosporin A and acetaminophen (Fig. 2) may be derived from outside of mitochondrial compartment. Moreover, biliary excretion of GSSG in this group was higher than other groups (control, 1.85±0.21; cyclosporin A, 2.43±0.46; acetaminophen, 1.97±0.26; cyclosporin A+acetaminophen, 4.67±0.44 nmol/min), whereas that of GSH was unchanged (control, 6.26±0.86; cyclosporin A, 6.42±1.19; acetaminophen, 5.60±0.75; cyclosporin A+acetaminophen, 5.39±1.44 nmol/min). Because GSSG accumulated in the mitochondrial compartment is not released into bile [33], these data support the idea that the increase in liver GSSG at 24 h after the treatment with cyclosporin A and acetaminophen is attributable to the extramitochondrial oxidative stress, which is irrelevant for the liver injury.

Depletion of mitochondrial ATP, which is likely more critical event for the toxicity, was observed in the acetaminophen-treated mice and was also partially prevented in the mice treated with cyclosporin A (Fig. 3). Because mitochondrial oxidative stress and the depletion of ATP has been implicated with MPT [34], the beneficial effects of cyclosporin A support our conclusion that MPT is a key step in the acetaminophen-induced liver injury. Leakage of cytochrome c into cytosol, which is correlated with MPT and a signal for apoptotic cell death, was detected in the acetaminophen-treated mice and was slightly attenuated by the coadministration of cyclosporin A (Fig. 4). This result also demonstrates the opening of the cyclosporin-sensitive MPT pore in the acetaminophen hepatotoxicity. MPT is characterized by a progressive permeabilization of the inner mitochondrial membrane dependent on the excessive amount of intramitochondrial Ca^{2+} and results in mitochondrial swelling [16,17]. Energized mitochondria from control mice tolerated Ca^{2+} at the concentration of 20 μM without undergoing the MPT as assessed by mitochondrial swelling (Fig. 5). By contrast, mitochondria from acetaminophen-treated mice were much more sensitive to the MPT induction. A large-amplitude swelling was observed with mitochondria from the treated mice and was prevented by the addition of cyclosporin A (1 μM) into the reaction medium (Fig. 5).

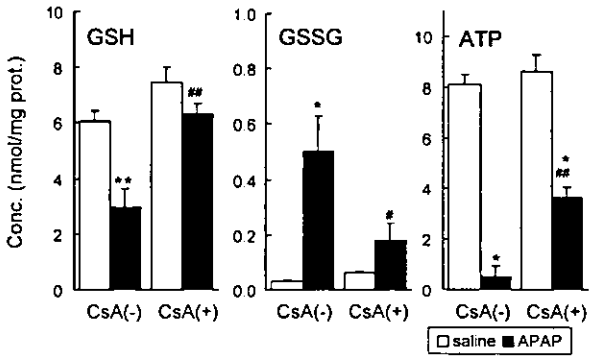

Fig. 3. Mitochondrial GSH, GSSG and ATP contents after administration of acetaminophen. Mice were given acetaminophen (APAP, 350 mg/kg, i.p.) together with or without cyclosporin A (CsA, 50 mg/kg, i.p.), and were killed 8 h after the treatment. Contents of GSH, GSSG and ATP in liver mitochondria were determined. The results are means±SE of 3–6 mice. *$P<0.05$, **$P<0.01$, Significantly different from corresponding APAP(−) groups. #$P<0.05$, ##$P<0.01$, Significantly different from corresponding CsA(−) groups.

3.3. In vitro effects of acetaminophen and NAPQI on isolated mitochondria

Incubation of energized mitochondria in the presence of Ca^{2+} (20 μM) and NAPQI (5–50 μM) induced a large-

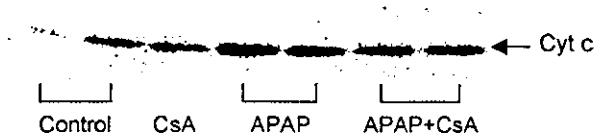

Fig. 4. Leakage of cytochrome c to cytosol after administration of acetaminophen. Mice were given acetaminophen (350 mg/kg, i.p.) together with or without cyclosporin A (50 mg/kg, i.p.), and were killed 24 h after the treatment. Hepatic cytosol fractions from the mice were analyzed by Western blot analysis with antibody against cytochrome c. Each lane represents a sample from a single mouse. The results are representative blots from 3 to 5 mice.

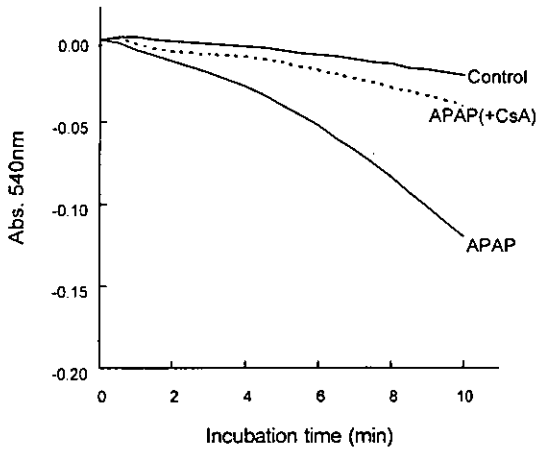

Fig. 5. Swelling of liver mitochondria from mice after administration of acetaminophen. Mice were given acetaminophen (350 mg/kg, i.p.) and were killed 8 h after the treatment along with control mice. Mitochondria (1 mg/ml) of the mice were incubated in the reaction medium containing 125 mM sucrose, 150 mM KCl, 10 mM HEPES-KOH, 2.5 μM rotenone, 20 μM $CaCl_2$, and was energized by 5 mM succinate. Absorbance at 540 nm was monitored after adding $CaCl_2$. The dotted line shows the incubation of mitochondria from acetaminophen-treated mice with 1 μM cyclosporin A. The results are representatives from 3 to 5 experiments.

amplitude swelling (Fig. 6). Addition of cyclosporin A (1 μM) prevented the mitochondrial swelling induced by NAPQI. On the other hand, acetaminophen did not induce swelling at the acetaminophen concentration up to 5 mM

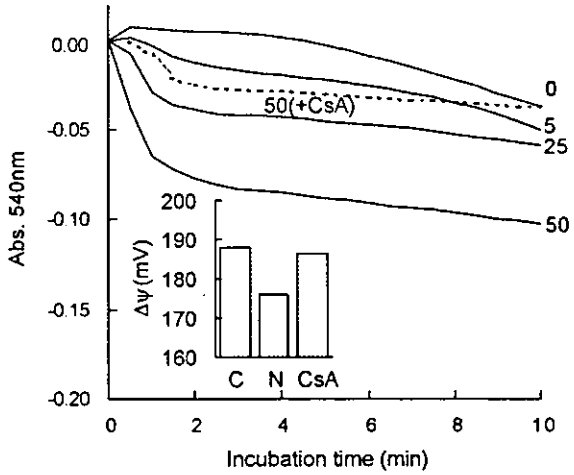

Fig. 6. Swelling and depolarization of liver mitochondria from mice in vitro treated with NAPQI. Mitochondria (1 mg/ml) of untreated mice were incubated in the reaction medium containing 125 mM sucrose, 150 mM KCl, 10 mM HEPES-KOH, 2.5 μM rotenone, 20 μM $CaCl_2$, 5–50 μM NAPQI and were energized by 5 mM succinate. Absorbance at 540 nm was monitored after adding NAPQI. Numbers in the figure are concentrations (μM) of NAPQI. The dotted line shows the incubation of mitochondria with 50 μM NAPQI and 1 μM cyclosporin A. The plots inserted are $\Delta\psi$ values obtained from the fluorescence intensity at the 505/535 nm wavelength pair after incubation of the same mixture with 0.5 mM rhodamine 123. The addition of chemicals (C, no addition; N, 50 μM NAPQI; CsA, 50 μM NAPQI+1 μM cyclosporin A) are shown in the bottom. The results are representatives of 3 experiments.

(data not shown). The transmembrane potential of mitochondria energized with succinate was assessed in the presence of Ca^{2+} by using a cationic dye, rhodamine 123 as an indicator. Incubation of mitochondria with NAPQI (50 μM) caused a decrease in membrane potential in the presence of Ca^{2+} and the mitochondrial depolarization was also prevented by the addition of cyclosporin A (Fig. 6 insert).

4. Discussion

The present study demonstrates that in vivo treatment of male CD-1 mice with acetaminophen results in MPT and suggests that the MPT is involved in pathogenesis of acetaminophen-induced liver injury. Although a number of mitochondrial proteins have been identified as targets of covalent binding of NAPQI, a reactive metabolite of acetaminophen [8,9], the pathogenic role of the covalent binding in the toxicity has not been fully elucidated. On the other hand, MPT was recently proposed as a mechanism of the acetaminophen hepatotoxicity associated with the covalent binding [21,22]. Indeed, the other reports presented protective effect of cyclosporin A against the acetaminophen toxicity [35,36]. However, one of them observed the protective effect of combination of cyclosporin A, fructose and trifluoperazine against acetaminophen hepatotoxicity [35], and thus the contribution of blocking MPT to the overall protection remains unknown. Another assessed the systemic toxicity (LD_{50}) but not liver injury as in vivo toxicity of acetaminophen [36]. Therefore, the present data indicating that cyclosporin A protected mice against acetaminophen-induced liver injury is the first report to demonstrate the in vivo pathogenic role of MPT in the hepatotoxicity of acetaminophen.

Several mechanisms may underlie acetaminophen-induced, probably NAPQI-mediated MPT. MPT pore constitutes a complex assembly of voltage-dependent anion channel in the outer membrane, adenine nucleotide translocase in the inner membrane and cyclophilin D in the matrix [34]. None of these proteins has reported to be a direct target of the covalent binding of NAPQI, allowing us to postulate the oxidative damage of the mitochondrial membrane protein(s) by NAPQI, because it possesses oxidant characteristics [37]. Indeed, it has been reported that mitochondrial NADPH and protein thiols were oxidized by NAPQI [38]. If the membrane thiol is oxidized, essentially thiol cross-linkage is formed, the conformation is changed, followed by opening of the pore. Adenine translocator has been proposed as a protein to form cross-linkage [39]. It was reported that late treatment of acetaminophen-treated mouse hepatocytes with dithiothreitol, a thiol-reducing agent, but not *N*-acetylcysteine prevented the liver injury [40], suggesting that reversal of an oxidation state, which increases the probability of the open state of the pore, is effective for the hepatoprotection.

On the other hand, the voltage-dependent regulation of the MPT pore has been characterized by depolarization of the membrane ant resultant increase in probability of the pore opening. An important factor determining the voltage gating potential of the MPT pore is also redox state of vicinal cysteine thiols, which are closely associated with the voltage-sensing element of the MPT pore [41]. These findings suggest the mitochondrial oxidative stress is responsible for occurrence of MPT. Furthermore, it was reported that NAPQI was able to raise cell calcium probably by inhibition of plasma membrane Ca^{2+}-ATPase through its depleting effect on GSH and protein-bound SH groups [10]. The increase in cellular Ca^{2+} in vivo should sensitize liver mitochondria to NAPQI-induced MPT pore opening.

Various changes caused by MPT and associated with toxicity are presented, which include membrane depolarization, uncoupling of oxidative phosphorylation, and release intramitochondrial ions and metabolic intermediates [10]. Among them, MPT as a source of superoxide was proposed to be an important event in acetaminophen hepatotoxicity [21,22]. The generation of superoxide supports the theory that oxidative stress in addition to covalent binding is involved in the acetaminophen hepatotoxicity. In the present study, acetaminophen-induced mitochondrial oxidative stress was suppressed by cyclosporin A (Fig. 3). It is thus suggested that the mitochondrial oxidative damage is the result of MPT, as well as the cause of MPT as described above. Furthermore, depletion of mitochondrial ATP in the acetaminophen-treated mice was also attenuated by cyclosporin A (Fig. 3), which occurs as a result of the MPT [34]. Recent studies have suggested that nitric oxide (NO) as well as superoxide is involved in the acetaminophen-induced liver injury [42,43]. NO is known to trap superoxide and generate peroxynitrite, which is highly reactive and toxic. Because peroxynitrite also induces MPT [44], the MPT may provide the mechanism how NO participates in the acetaminophen hepatotoxicity, although we have not investigated NO-dependent pathways in the present study.

We detected leakage of cytochrome c into cytosol in the acetaminophen-treated mice, which is correlated with MPT pore opening (Fig. 4). The leakage were slightly attenuated by cyclosporin A, supporting our conclusion that the protection against acetaminophen hepatotoxicity is accounted for by the protection against MPT. Furthermore, leakage of cytochrome c implies induction of apoptosis because cytochrome c is known to be a signal of apoptosis cascade by activating caspases such as caspase 9 and then caspase 3 [45]. Acetaminophen could induce hepatocyte apoptosis in vitro as well as necrosis, whereas the quantitative determination of cell death after exposure of hepatotoxic dose of acetaminophen in vivo indicated that acetaminophen caused extensively oncotic necrosis rather than apoptosis [20]. Thus, it is reasonable to postulate that necrotic cell death is mainly induced also in the present study, although we have not determined the type of cell death. It is considered that depletion of ATP induced by the MPT and by other events prevents the apoptotic cell death, which requires ATP [46], in acetaminophen-induced liver injury. On the other hand, it was recently reported that although caspases and apoptosis were important in initiating the acetaminophen-induced liver injury, the apoptotic pathway was only incompletely activated in response to acetaminophen treatment, and instead it degenerated to induce premature secondary necrosis [47].

In conclusion, MPT can explain the mechanism for acetaminophen-induced liver injury in vivo in mice, which is based on the consensus that mitochondria are the important target in the acetaminophen hepatotoxicity. NAPQI is considered to play an important role in the MPT. Suppression of the MPT resulted in protection not only from acetaminophen-induced liver injury but also from the known events closely related to the pathogenesis in the hepatotoxicity. Because the MPT is down-stream of covalent binding of NAPQI to the hepatocellular targets and linked with the secondary oxidative stress, it is suggested that blocking MPT should be a strategy for development of therapeutic agent for the acetaminophen overdose, which can be administrated later than *N*-acetylcysteine, which contributes to detoxify NAPQI.

Acknowledgements

This study was supported in part by a grant-in-aid from the Ministry of Education, Science and Culture of Japan.

References

[1] Mitchell JR, Jollow DJ, Potter WZ, Davis DC, Gillette JR, Brodie BB. Acetaminophen-induced hepatic necrosis. I. Role of drug metabolism. J Pharmacol Exp Ther 1973;187:185–194.

[2] Dahlin DC, Miwa GT, Lu AY, Nelson SD. *N*-Acetyl-*p*-benzoquinone imine: a cytochrome P-450-mediated oxidation product of acetaminophen. Proc Natl Acad Sci USA 1984;81:1327–1331.

[3] Jollow DJ, Mitchell JR, Potter WZ, Davis DC, Gillette JR, Brodie BB. Acetaminophen-induced hepatic necrosis. II. Role of covalent binding in vivo. J Pharmacol Exp Ther 1973;187:195–202.

[4] Mitchell JR, Jollow DJ, Potter WZ, Gillette JR, Brodie BB. Acetaminophen-induced hepatic necrosis. IV. Protective role of glutathione. J Pharmacol Exp Ther 1973;187:211–217.

[5] Manautou JE, Emeigh Hart SG, Khairallah EA, Cohen SD. Protection against acetaminophen hepatotoxicity by a single dose of clofibrate: effects on selective protein arylation and glutathione depletion. Fundam Appl Toxicol 1996;29:229–237.

[6] Tarloff JB, Khairallah EA, Cohen SD, Goldstein RS. Sex- and age-dependent acetaminophen hepato- and nephrotoxicity in Sprague–Dawley rats: role of tissue accumulation, nonprotein sulfhydryl depletion, and covalent binding. Fundam Appl Toxicol 1996;30: 13–22.

[7] Schnellmann JG, Pumford NR, Kusewitt DF, Bucci TJ, Hinson JA. Deferoxamine delays the development of the hepatotoxicity of acetaminophen in mice. Toxicol Lett 1999;106:79–88.

[8] Cohen SD, Pumford NR, Khairallah EA, Boekelheide K, Pohl LR, Amouzadeh HR, et al. Selective protein covalent binding and target organ toxicity. Toxicol Appl Pharmacol 1997;143:1–12.

[9] Qiu Y, Benet LZ, Burlingame AL. Identification of the hepatic protein targets of reactive metabolites of acetaminophen in vivo in mice using two-dimensional gel electrophoresis and mass spectrometry. J Biol Chem 1998;273:17940–17953.
[10] Moore M, Thor H, Moore G, Nelson S, Moldeus P, Orrenius S. The toxicity of acetaminophen and *N*-acetyl-*p*-benzoquinone imine in isolated hepatocytes is associated with thiol depletion and increased cytosolic Ca^{2+}. J Biol Chem 1985;260:13035–13040.
[11] Burcham PC, Harman AW. Acetaminophen toxicity results in site-specific mitochondrial damage in isolated mouse hepatocytes. J Biol Chem 1991;266:5049–5054.
[12] Harman AW, Kyle ME, Serroni A, Farber JL. The killing of cultured hepatocytes by *N*-acetyl-*p*-benzoquinone imine (NAPQI) as a model of the cytotoxicity of acetaminophen. Biochem Pharmacol 1991;41: 1111–1117.
[13] Nazareth WM, Sethi JK, McLean AE. Effect of paracetamol on mitochondrial membrane function in rat liver slices. Biochem Pharmacol 1991;42:931–936.
[14] Parmar DV, Ahmed G, Khandkar MA, Katyare SS. Mitochondrial ATPase: a target for paracetamol-induced hepatotoxicity. Eur J Pharmacol 1995;293:225–229.
[15] Gupta S, Rogers LK, Taylor SK, Smith CV. Inhibition of carbamyl phosphate synthetase-I and glutamine synthetase by hepatotoxic doses of acetaminophen in mice. Toxicol Appl Pharmacol 1997;146: 317–327.
[16] Bernardi P. The permeability transition pore control points of a cyclosporin A-sensitive mitochondrial channel involved in cell death. Biochim Biophys Acta 1996;1275:5–9.
[17] Lemasters JJ, Nieminen AL, Qian T, Trost LC, Elmore SP, Nishimura Y, et al. The mitochondrial permeability transition in cell death: a common mechanism in necrosis, apoptosis and autophagy. Biochim Biophys Acta 1998;1366:177–196.
[18] Masubuchi Y, Nakayama S, Horie T. Role of mitochondrial permeability transition in diclofenac-induced hepatocyte injury in rats. Hepatology 2002;35:544–551.
[19] Zoratti M, Szabo I. The mitochondrial permeability transition. Biochim Biophys Acta 1995;1241:139–176.
[20] Gujral JS, Knight TR, Farhood A, Bajt ML, Jaeschke H. Mode of cell death after acetaminophen overdose in mice: apoptosis or oncotic necrosis? Toxicol Sci 2002;67:322–328.
[21] Jaeschke H, Knight TR, Bajt ML. The role of oxidant stress and reactive nitrogen species in acetaminophen hepatotoxicity. Toxicol Lett 2003;144:279–288.
[22] James LP, McCullough SS, Lamps LW, Hinson JA. Effect of *N*-acetylcysteine on acetaminophen toxicity in mice: relationship to reactive nitrogen and cytokine formation. Toxicol Sci 2003;75: 458–467.
[23] Schneider WC, Hogeboom GH. Intracellular distribution of enzymes. V. Further studies on the distribution of cytochrome c in liver homogenate. J Biol Chem 1950;183:123–128.
[24] Lowry OH, Rosebrough NJ, Farr AL, Randall RJ. Protein measurement with the folin phenol reagent. J Biol Chem 1951;193:265–275.
[25] Keller DA, Menzel DB. Picomole analysis of glutathione, glutathione disulfide, glutathione S-sulfonate, and cysteine S-sulfonate by high-performance liquid chromatography. Anal Biochem 1985;151: 418–423.
[26] Emaus RK, Grunwald R, Lemasters JJ. Rhodamine 123 as a probe of transmembrane potential in isolated rat-liver mitochondria: spectral and metabolic properties. Biochim Biophys Acta 1986;850:436–448.
[27] Berg-Candolfi M, Candolfi E, Benet LZ. Suppression of intestinal and hepatic cytochrome P4503A in murine toxoplasma infection Effects of *N*-acetylcysteine and *N*(G)-monomethyl-L-arginine on the hepatic suppression. Xenobiotica 1996;26:381–394.
[28] Lee SS, Buters JT, Pineau T, Fernandez-Salguero P, Gonzalez FJ. Role of CYP2E1 in the hepatotoxicity of acetaminophen. J Biol Chem 1996;271:12063–12067.
[29] Sinclair JF, Szakacs JG, Wood SG, Walton HS, Bement JL, Gonzalez FJ, et al. Short-term treatment with alcohols causes hepatic steatosis and enhances acetaminophen hepatotoxicity in Cyp2e1(−/−) mice. Toxicol Appl Pharmacol 2000;168:114–122.
[30] Zhang J, Huang W, Chua SS, Wei P, Moore DD. Modulation of acetaminophen-induced hepatotoxicity by the xenobiotic receptor CAR. Science 2002;298:422–424.
[31] Wolf A, Trendelenburg CF, Diez-Fernandez C, Prieto P, Houy S, Trommer WE, et al. Cyclosporine A-induced oxidative stress in rat hepatocytes. J Pharmacol Exp Ther 1997;280:1328–1334.
[32] Knight TR, Kurtz A, Bajt ML, Hinson JA, Jaeschke H. Vascular and hepatocellular peroxynitrite formation during acetaminophen toxicity: role of mitochondrial oxidant stress. Toxicol Sci 2001;62:212–220.
[33] Jaeschke H. Glutathione disulfide formation and oxidant stress during acetaminophen-induced hepatotoxicity in mice in vivo: the protective effect of allopurinol. J Pharmacol Exp Ther 1990;255:935–941.
[34] Kim JS, He L, Lemasters JJ. Mitochondrial permeability transition: a common pathway to necrosis and apoptosis. Biochem Biophys Res Commun 2003;304:463–470.
[35] Beales D, McLean AE. Protection in the late stages of paracetamol-induced liver cell injury with fructose, cyslosporin A and trifluoperazine. Toxicology 1996;107:201–208.
[36] Haouzi D, Cohen I, Vieira HL, Poncet D, Boya P, Castedo M, et al. Mitochondrial permeability transition as a novel principle of hepatorenal toxicity in vivo. Apoptosis 2002;7:395–405.
[37] Powis G, Svingen BA, Dahlin DC, Nelson SD. Enzymatic and non-enzymatic reduction of *N*-acetyl-*p*-benzoquinone imine and some properties of the *N*-acetyl-*p*-benzosemiquinone imine radical. Biochem Pharmacol 1984;33:2367–2370.
[38] Weis M, Moore GA, Cotgreave IA, Nelson SD, Moldeus P. Quinone imine-induced Ca^{2+} release from isolated rat liver mitochondria. Chem Biol Interact 1990;76:227–240.
[39] Brustovetsky N, Klingenberg M. Mitochondrial ADP/ATP carrier can be reversibly converted into a large channel by Ca^{2+}. Biochemistry 1996;35:8483–8488.
[40] Grewal KK, Racz WJ. Intracellular calcium disruption as a secondary event in acetaminophen-induced hepatotoxicity. Can J Physiol Pharmacol 1993;71:26–33.
[41] Petronilli V, Costantini P, Scorrano L, Colonna R, Passamonti S, Bernardi P. The voltage sensor of the mitochondrial permeability transition pore is tuned by the oxidation-reduction state of vicinal thiols. Increase of the gating potential by oxidants and its reversal by reducing agents. J Biol Chem 1994;269:16638–16642.
[42] Bourdi M, Masubuchi Y, Reilly TP, Amouzadeh HR, Martin JL, George JW, et al. Protection against acetaminophen-induced liver injury and lethality by interleukin 10: role of inducible nitric oxide synthase. Hepatology 2002;35:289–298.
[43] Gardner CR, Laskin JD, Dambach DM, Sacco M, Durham SK, Bruno MK, et al. Reduced hepatotoxicity of acetaminophen in mice lacking inducible nitric oxide synthase: potential role of tumor necrosis factor-alpha and interleukin-10. Toxicol Appl Pharmacol 2002;184:27–36.
[44] Radi R, Cassina A, Hodara R, Quijano C, Castro L. Peroxynitrite reactions and formation in mitochondria. Free Radic Biol Med 2002; 33:1451–1464.
[45] Cai J, Yang J, Jones DP. Mitochondrial control of apoptosis: the role of cytochrome c. Biochim Biophys Acta 1998;1366:139–149.
[46] Eguchi Y, Shimizu S, Tsujimoto Y. Intracellular ATP levels determine cell death fate by apoptosis or necrosis. Cancer Res 1997;57:1835–1840.
[47] El-Hassan H, Anwar K, Macanas-Pirard P, Crabtree M, Chow SC, Johnson VL, et al. Involvement of mitochondria in acetaminophen-induced apoptosis and hepatic injury: roles of cytochrome c, Bax, Bid, and caspases. Toxicol Appl Pharmacol 2003;191:118–129.

JOURNAL OF VIROLOGY, Oct. 2004, p. 10820–10824 Vol. 78, No. 19
0022-538X/04/$08.00+0 DOI: 10.1128/JVI.78.19.10820–10824.2004

Identification of Basal Promoter and Enhancer Elements in an Untranslated Region of the TT Virus Genome

Tetsuro Suzuki,[1]* Ryosuke Suzuki,[1] Jin Li,[1] Minako Hijikata,[2] Mami Matsuda,[1] Tiang-Cheng Li,[1] Yoshiharu Matsuura,[3] Shunji Mishiro,[4] and Tatsuo Miyamura[1]

Department of Virology II, National Institute of Infectious Diseases,[1] and Department of Respiratory Diseases, Research Institute, International Medical Center of Japan,[2] Shinjuku-ku, and Department of Medical Sciences, Toshiba General Hospital, Shinagawa-ku,[4] Tokyo, and Research Center for Emerging Infectious Diseases, Research Institute for Microbial Diseases, Osaka University, Suita-shi, Osaka,[3] Japan

Received 2 April 2004/Accepted 19 May 2004

The regulation of TT virus (TTV) gene expression was characterized. Transient-transfection assays using reporter constructs revealed that a 113-nucleotide (nt) sequence within the untranslated region, proximal to the transcription initiation site and containing a TATA box motif, has a basal promoter activity. This sequence is well conserved among different TTV genotypes. Upstream stimulating factor bound to a consensus binding motif within this region and positively regulates TTV transcription. Furthermore, a 488-nt region upstream of the basal promoter exhibited enhancer activity, presumably in a cell type-specific manner. This study illustrates some of the mechanisms involved in the transcriptional regulation of TTV.

TT virus (TTV), which was discovered in a patient with acute hepatitis, is an unenveloped, single-stranded, circular DNA virus, with a genome of approximately 3.8 kb (6). TTV is thought to be a new member of the *Circoviridae* family of viruses, and it was recently proposed that the virus be named Torque Teno virus (6). The TTV genome includes an untranslated region (UTR) of approximately 1.2 kb and a coding region of approximately 2.6 kb, including two major open reading frames which are sandwiched by the TATA box and polyadenylation signal motifs (11, 13, 15). Analyses of TTV transcripts have revealed three spliced mRNA species of 3.0, 1.2, and 1.0 kb with common 5′ and 3′ termini (9, 14). However, the molecular mechanisms controlling TTV transcription are still unknown. In this study, the basal promoter and enhancer of a TTV isolate, SANBAN of genogroup 3 (5, 18), were identified and functionally characterized.

First, we determined the transcription initiation sites of the TTV genome by 5′ rapid amplification of cDNA end (5′-RACE) analysis (Marathon cDNA amplification kit; Clontech) using poly(A)-rich RNA from a human hepatocellular carcinoma cell line, HepG2, transfected with a cloned TTV genome. The 5′-RACE PCR products were cloned and sequenced. We observed two potential transcription initiation sites, which map at nucleotides (nt) 121 and 110 (numbered according to the sequence deposited in DDBJ/GenBank/EMBL databases under accession number AB025946). Although transcription may be initiated at both sites, the upper site was designated position +1 in this study.

The UTR of the TTV genome contains a TATA box element between positions −40 and −35, as well as a number of putative transcription factor-binding motifs (Fig. 1A). Despite considerable genetic diversity throughout the whole genome, the UTR sequence was relatively conserved among the different TTV genotypes, presumably reflecting its functional constraints (15, 16). Thus, we analyzed transcriptional regulation of the UTR sequence.

To characterize TTV promoter activity, a firefly luciferase reporter plasmid, p(−890/+115), was constructed by subcloning the TTV sequence from positions −890 to +115, which was amplified by PCR using appropriate primers with restriction sites at the 5′ ends, into the promoterless pGL3-Basic (Promega). Eleven different cell lines were transfected with p(−890/+115), along with a *Renilla* luciferase expression vector, pRL-TK, as an internal standard for determining transfection efficiency. Luciferase activities in cell lysates prepared after 16 h of transfection were determined (2). It is of interest that the 1.0-kb fragment demonstrated a pronounced promoter activity in all the hepatocellular carcinoma cell lines tested. Human (Huh7, HepG2, and FLC4 [1, 2]) and mouse (Hepa1-clc7) hepatocellular carcinoma cells were tested (Fig. 1B). This fragment demonstrated the greatest activity in Huh7 cells (~10-fold greater than in other cells). We observed substantial promoter activity in GL37 (African green monkey kidney) and CHO (Chinese hamster ovary) cells, whereas limited activity was observed in Caco2 (human colon carcinoma), MOLT4 (human T-cell leukemia), CV1 (African green monkey kidney fibroblast), 3T3 Swiss (mouse fibroblast), and CMT93 (mouse rectal carcinoma) cells. These results indicate that the UTR of the TTV genome functions as a promoter in a cell type-specific manner.

To assess basal, proximal promoter activity in the UTR, a series of 5′ deletions fused to the luciferase gene were constructed and transfected into Huh7 and HepG2 cells (Fig. 2). A deletion extending to nt −601 [p(−601/+115)] enhanced promoter activity in both cell lines (by ~1.5-fold), while deletion of another 274 nt [p(−327/+115)] decreased promoter activity by more than 80%, suggesting that there is a negative regula-

* Corresponding author. Mailing address: Department of Virology II, National Institute of Infectious Diseases, 1-23-1 Toyama, Shinjuku-ku, Tokyo 162-8640, Japan. Phone: (81) 3-5285-1111. Fax: (81) 3-5285-1161. E-mail: tesuzuki@nih.go.jp.